Spatial Resolution Enhancement in a 2D Photonic Crystal Based on Complex Square Lattice

Somayeh Rafiee Dastjerdi[a], Majid Ghanaatshoar[a, b], and Kaveh Delfanazari[c]

[a]Laser and Plasma Research Institute, Shahid Beheshti University, G.C., Evin 1983969411, Tehran, Iran
[b]Solar Cells Research Group, Shahid Beheshti University, G.C., Evin 1983969411, Tehran, Iran
[c]Optoelectronic Research Centre, University of Southampton, SO17 1BJ, Southampton, UK

***Corresponding Author:** m-ghanaat@cc.sbu.ac.ir

Abstract— We study the focusing properties of a two dimensional complex square-lattice photonic crystal (PC) comprising air holes immersed in Ge medium. The finite difference time domain (FDTD) method is utilized to calculate the dispersion band diagram and to simulate the image formation incorporating the perfectly matched layer (PML) boundary condition. In contrast to the common square PCs with the same air filling factor, the frequency corresponding to the effective negative refraction occurs in the second photonic band and the spatial image resolution is improved.

Keywords: 2D photonic crystal, Integrated optics, Near-field imaging, Negative index materials, Sub-wavelength spatial resolution.

I. INTRODUCTION

In 1968 Veselago analyzed the material with simultaneously negative permeability and permittivity and theoretically showed that such a material should possess a negative refractive index. Regarding to the opposite direction of the pointing and the wave vectors in these materials, he called them left-handed materials (LHMs) [1]. Currently such a meta-material has attracted a lot of attention due to anomalous behavior that has potential to develop biomedical imaging, optical communications and optoelectronic technologies [2- 8]. These materials are able to restore both the phase of propagating waves and amplitude of the evanescent waves to make a perfect lens which can overcome the diffraction limit of conventional convex lenses [9]. Photonic crystals (PCs) as a human-made structures are able to explore the effective negative index of refraction in the infra-red and optical frequencies. In contrast to the conventional lenses in which imaging effects obey the Newton's formula, in PCs the imaging is related to mirror-inversion transformation, like as mirrors but with respect to this fact that the PCs produce real images [10]. Furthermore, there is no need to form a curved surface to obtain an image and also we can attain sub-wavelength imaging free from the diffraction limits [9].

PCs which are constructed from dielectric constituents, with positive permeability and permittivity, can perform the imaging with respect to the effective negative refractive index or the channeling effect at visible and infrared frequency regimes. For instance, 2D triangular, hexagonal and honeycomb high symmetric PCs can be realized as a left-handed material in the frequency which is belong to the second energy band with negative group velocity [11, 12]. On the other hand, in PCs based on the square lattices, the negative refraction effect occurs in the region of the first photonic band where an isotropic negative index cannot be defined. In fact, for the frequencies belonging to the first energy band, production sign of the Poynting vector (S) and the wave vector (k) will be positive and the PC behaves as a right-handed material. In this case, the image formation is reached by anisotropy or higher-order Bragg scattering effect [13]. Negative refraction effect of the 2D square lattices in the second photonic band has been observed experimentally in the range of microwave frequencies [14].

In this work, we propose a 2D square lattice photonic crystal consisting of the air holes in the dielectric medium. We show that this PC with a complex lattice structure can be regarded as a near-field superlensing device which can work at near-infrared regime based on the negative refraction effect. In addition, based on the Rayleigh criterion, we illustrate the spatial resolution enhancement of this super-lens. The finite difference time domain (FDTD) method with periodic boundary condition is utilized to calculate the dispersion band diagram of the PC and the FDTD method incorporating the perfectly matched layer (PML) boundary condition is used to simulate the field pattern of the point sources and images.

II. Band Diagram Specifications

The PC proposed here is a 2D faced-centered square lattice consisting of periodic arrays of infinitely long, cylindrical air holes immersed in germanium medium as schematically shown in Fig. 1. Dielectric constant of Ge at λ=1.55 μm is ε_{Ge}=18 and the radii of holes are assumed to be R_1=0.25*a* and R_2=0.15*a*, where "*a*" is the lattice constant. In the meantime, we assume that the width of the PC in the x direction is limited and in the y direction is unrestricted.

Based on the structure of this PC, we consider the transverse electric (TE) polarization of electromagnetic (EM) wave and employ the FDTD method based on the common Yee's algorithm to obtain the band diagram of the PC along the most symmetrical lines (ΓX, XM, MΓ) in the first Brillouin zone. The FDTD is a method based on an algorithm that calculates the temporal evolvement of the EM fields [15].

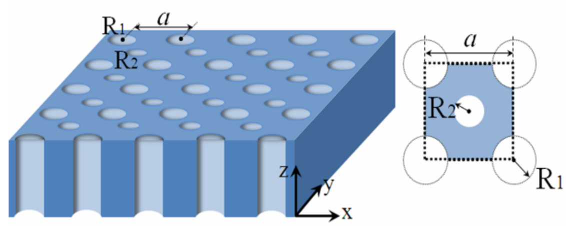

Fig. 1. (left) Schematic view and (right) the unit cell of the 2D complex square lattice PC formed by air holes in germanium with radii R_1 and R_2 and the lattice constant *a*.

The time dependent Maxwell's equations in a linear, isotropic and non-dispersive material can be written as:

$$\nabla \times \mathbf{E} = -\mu(\mathbf{r})\,\partial \mathbf{H}/\partial t, \qquad (1)$$
$$\nabla \times \mathbf{H} = \varepsilon(\mathbf{r})\,\partial \mathbf{E}/\partial t,$$

where ε and μ are the permittivity and permeability of the material, respectively. Taking the central difference approximation for both spatial and temporal derivatives gives:

$$H_z\Big|_{i,j,k}^{n+1/2} = H_z\Big|_{i,j,k}^{n-1/2} - \frac{\Delta t}{\mu_{i,j,k}}\left[\frac{E_y\Big|_{i+1,j,k}^{n} - E_y\Big|_{i,j,k}^{n}}{\Delta x} - \frac{E_x\Big|_{i,j+1,k}^{n} - E_x\Big|_{i,j,k}^{n}}{\Delta y}\right],$$

$$E_x\Big|_{i,j,k}^{n+1} = E_x\Big|_{i,j,k}^{n} + \frac{\Delta t}{\varepsilon_{i,j,k}}\left[\frac{H_z\Big|_{i,j,k}^{n+1/2} - H_z\Big|_{i,j-1,k}^{n+1/2}}{\Delta y}\right], \qquad (2)$$

$$E_y\Big|_{i,j,k}^{n+1} = E_y\Big|_{i,j,k}^{n} + \frac{\Delta t}{\varepsilon_{i,j,k}}\left[\frac{H_z\Big|_{i,j,k}^{n+1/2} - H_z\Big|_{i-1,j,k}^{n+1/2}}{\Delta x}\right].$$

Once the cell size Δx is chosen properly, then the time step is determined by the well-known Courant condition:

$$\Delta t \leq \Delta x / (c\sqrt{n}), \quad (3)$$

where n is the dimension of the simulation and c is the speed of light in free space.

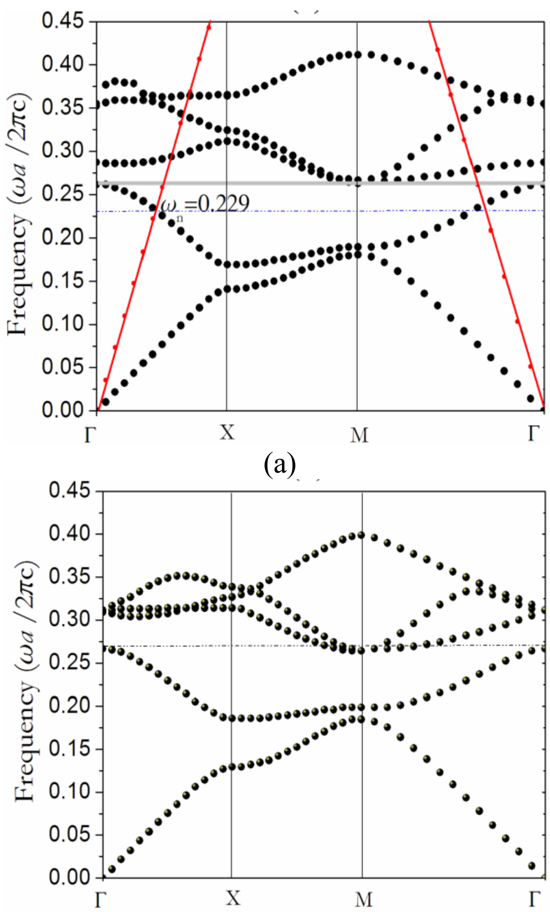

Fig. 2. Photonic band diagram of (a) a complex square lattice PC made of air holes with radii R_1=0.25a and R_2=0.15a in germanium for TE mode, and (b) a simple square lattice PC made of air holes with radius R=0.29a in germanium. The solid lines originated from Γ point depict the dispersion lines of air and the small gray region in (a) shows the bandgap of the complex square lattice PC.

In band structure calculation by means of the FDTD method, random initial condition is utilized to prevent missing any possible modes. It also needs sufficient amount of time to give enough accuracy. For attaining eigenmodes we choose various low-symmetry locations in the unit cell of the PC as probes to record the peaks of the Fourier transform of the complex field components in the time domain for a given propagation constant [16]. We should notice that probes at high-symmetry locations of the PC's unit cell are not able to detect all the eigenmodes.

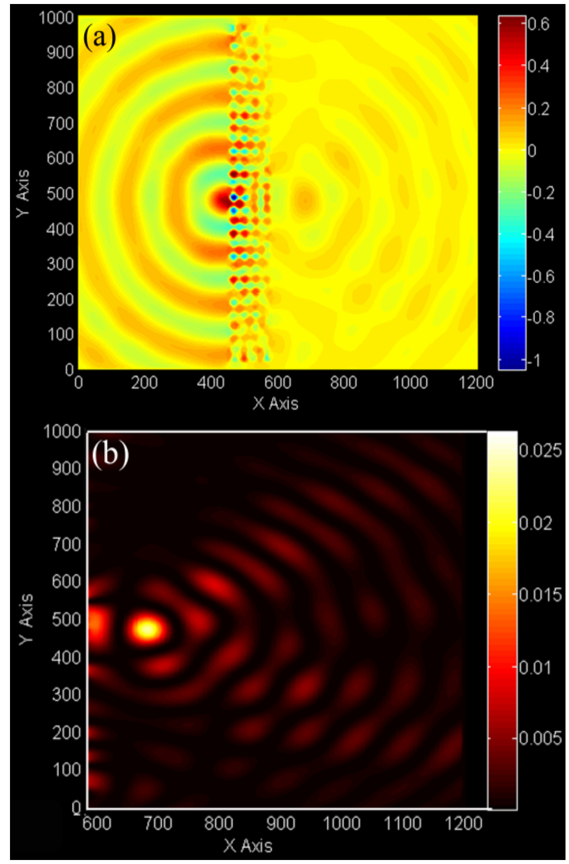

Fig. 3. (a) Magnetic field distribution of a point source at normalized frequency of 0.229 that is located 0.5a far from the left side of the 4.37a-thick PC, and (b) the corresponding magnetic field intensity on the right side of the PC structure.

Figure 2(a) displays the band diagram of the proposed structure, composed of air holes with radii R_1=0.25a and R_2=0.15a immersed in germanium medium and Fig. 2(b) illustrates the band diagram of the simple square lattice PC consisting of the air holes with radius R=0.29a. The two structures have the same air filling factor (0.27). In this figure, the frequency of EM wave is normalized by the factor $a/2\pi c$, where c is the speed of light in vacuum. By comparison, we pick out that the face-centered square lattice creates a 0.002(2πc/a) band gap between the second and the third energy bands and pushes the second band below the frequency 0.26(2πc/a).

To achieve the frequency at which the PC is able to show the effective negative refraction, we should pay attention to some important points. First of all, the frequency should be below $0.5\times2\pi c/a$ to avoid diffraction; secondly, the equi-frequency surface (EFS) of the PC around the Γ point should have an inward gradient leading to negative group velocity and finally, the PC's EFS should contain the EFS of the background [17, 18]. On the other hand, the existence of the negative refraction frequency near the band gap helps to be sure of this fact that our system can operate just in a specified frequency. We choose the frequency of the intersection point of the PC and air band diagrams to evaluate the imaging properties of this structure. The intersection normalized frequency, $\omega a/2\pi c$, is 0.229 and as it is apparent from Fig. 2(a), there is an inward gradient around the Γ point in this frequency.

For a given light wavelength (λ) and a fixed PC structure with lattice constant a, higher resolution is obtained by decreasing a/λ. Indeed, the lower the negative refraction frequency, the higher the image resolution of the PC lens [9]. In our system, this frequency is lower than the corresponding frequencies for the simple square and hexagonal PC lattices studied before [13, 19].

III. NEAR-FIELD IMAGE FORMATION

In order to simulate the image construction by proposed PC structure, we choose the intersection frequency $0.229(2\pi c/a)$ and utilize the FDTD method incorporating perfectly matched layer (PML) boundary condition for TE polarized EM wave. By considering the PC thickness as an integer multiple of the wavelength and mirror symmetry of the PC we can minimize the reflection from the whole structure. In this regard, we possess a $4.37a$-thick slab and fix the lattice constant to 355 nm to examine the imaging effect of the mentioned structure at near-infrared region.

We put a point source operating at 0.229 normalized frequency at distance $0.5a$ from the left side of the structure and calculate the magnetic field pattern of the point source and its image. Figure 3(a) and (b) illustrate the magnetic field pattern of TE-polarized wave through the PC and the corresponding magnetic field intensity at its right side. From this figure one can observe the image construction by the PC lens.

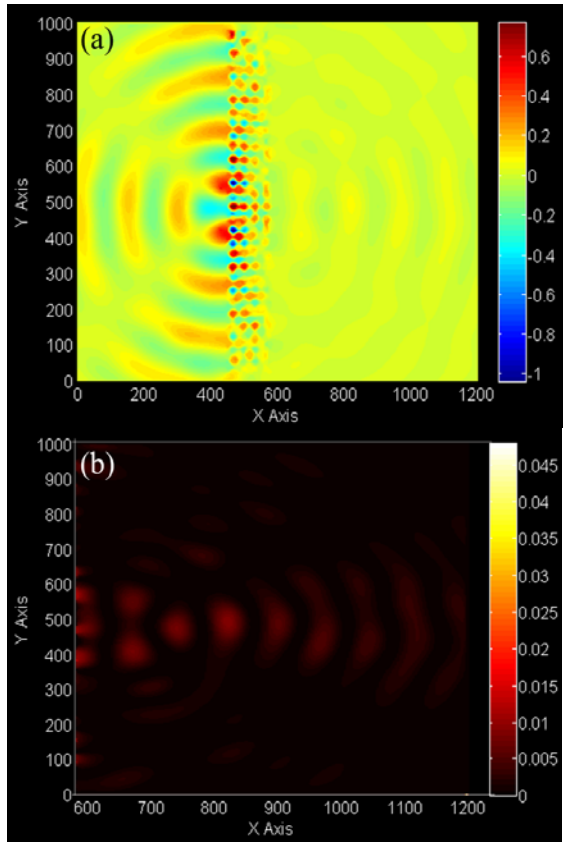

Fig. 4. (a) Magnetic field distribution at normalized frequency 0.229 of two point sources located at $0.5a$ from the left side of the PC that are separated by $3.5a$ from each other, and (b) the corresponding magnetic field intensity on the right side of the PC structure.

IV. SPATIAL RESOLUTION OF THE PC

Spatial resolution in optical systems determines how closely lines can be resolved in an image and so, higher resolution means more image details [20]. To investigate the spatial resolution of the considered structure, we put two point sources $0.5a$ away from the PC, where they are vertically separated by different distances.

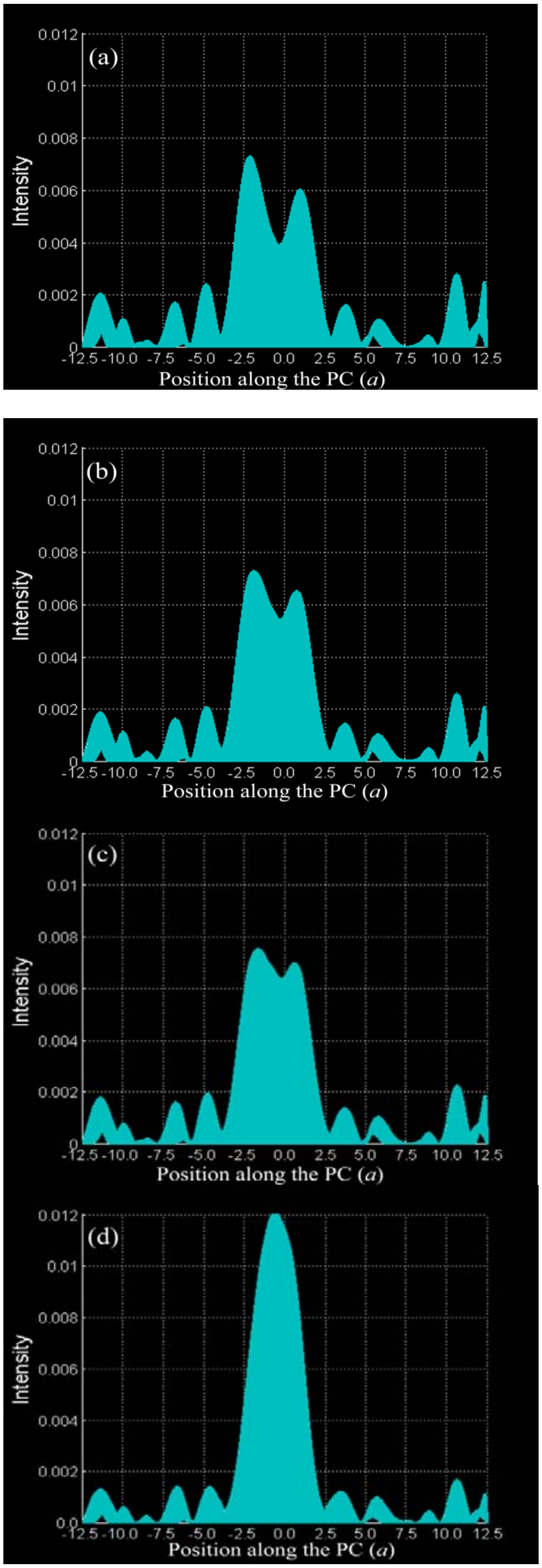

Fig. 5. Magnetic field intensity of the point sources located at 0.5*a* from the left side of the PC when they are separated vertically (a) 3.2*a*, (b) 3.1*a*, (c) 3.0*a* and (d) 2.9*a* from each other.

We assume that the point sources are coherent, so the resolution can be improved. For analyzing the spatial resolution of the PC lens we alter the distance between the point sources. Figure 4 depicts the magnetic field distribution and corresponding magnetic field intensity of light sources and their images when they are separated vertically 3.5*a* from each other. This figure shows clearly the images of the two point sources, but in order to gain the spatial resolution, it is not enough and we should still decrease the distance between the sources. So we start to decrease the distance between the sources from 3.5*a* to 2.9*a*.

According to Fig. 5, by reducing the distance between the sources to 2.9*a*, one can identify just one peak; whereas, for separation distance of 3*a*, two peaks of images can be resolved. In this case, by considering the Rayleigh criterion, the resolution of the system reaches 0.687λ which is improved compared with the results that have recently been achieved in a partitioned cylinder square lattice PC lens and an annular PC flat lens [13, 19].

V. Conclusion

Based on the band structure analysis, we investigated super-lensing behavior in a complex 2D square lattice PC consisting air holes immersed in the Ge medium. We found that this complex structure creates a compressed band diagram and opens the first frequency gap between the second and the third energy bands and fulfills all the conditions required for negative refraction effect. Compared to the conventional square lattice PCs, the frequency of negative refraction belongs to the second energy band and the spatial resolution of the structure is improved.

References

[1] V.G. Veselago, “The electromagnetic of substances with simultaneously negative value of ε and μ,” Sov. Phys. Usp. Vol. 10, pp. 509-514, 1968.

[2] L.Y.M. Tobing, L. Tjahjana, D.H. Zhang, Q. Zhang and Q. Xiong, “Deep subwavelength fourfold rotationally symmetric split-ring-resonator metamaterials for highly sensitive and robust biosensing platform," Sci. Rep. Vol. 3, pp. 02437 1-6), 2013.

[3] G. Dolling, C. Enkrich, M. Wegener, C. M. Soukoulis, and S. Linden, "Simultaneous negative phase and group velocity of light in a metamaterial," Science, Vol. 312, pp. 892–894, 2006.

[4] C.M. Lee, W.S. Shim, Y. Moon, and C.H. Seo, "Design of ultra-wide band-pass filter based on metamaterials applicable to microwave photonics," J. Opt. Soc. Korea, Vol. 16, pp. 288-291, 2012.

[5] M. Zedler, C. Caloz, and P. Russer, "A 3-D isotropic left-handed metamaterial based on the rotated transmission-line matrix scheme," IEEE Trans. Ant. Prop. Vol. 55, pp. 2930–2941, 2007.

[6] A.K. Iyer and G.V. Eleftheriades, "Mechanisms of subdiffraction free-space imaging using a transmission-line metamaterial superlens: An experimental verification," Appl. Phys. Lett. Vol. 92, p. 131105 (1-3), 2008.

[7] V.M. Shalaev, "Optical negative index metamaterials," Nature Photon. Vol. 1, pp. 41-48, 2007.

[8] J.M. Algarin, M.J. Freire, M.A. Lopez, M. Lapine, P.M. Jakob, V.C. Behr, and R. Marques, "Analysis of the resolution of split-ring metamaterial lenses with application in parallel magnetic resonance imaging," Appl. Phys. Lett. Vol. 98, pp. 014105 (1-3), 2011.

[9] J.B. Pendry, "Negative refraction makes a perfect lens," Phys. Rev. Lett. Vol. 85, pp. 3966-3969, 2000.

[10] M. Notomy, "Theory of light propagation in strongly modulated photonic crystals: refraction-like behavior in the vicinity of the photonic band gap," Phys. Rev. B, Vol. 62, pp. 10696-10705, 2000.

[11] J. Li, M.H. Lu, T. Fan, X.K. Liu, L. Feng, Y.F. Tang, and Y.F. Chen, "All-angle negative refraction imaging effect with complex two-dimensional hexagonal photonic crystals," J. Appl. Phys. Vol. 102, pp. 073538 (1-4), 2007.

[12] K.M. Lin and G.Y. Guo, "Uncoupled modes and all-angle negative refraction in walled honeycomb photonic crystals," J. Opt. Soc. Am. B, Vol. 25, pp. C75-C81, 2008.

[13] S.R. Dastjerdi, M. Ghanaatshoar, and T. Hattori, "Near-infrared subwavelength imaging and focusing analysis of a square lattice photonic crystal made from partitioned cylinders," J. Opt. Soc. Korea, Vol. 17, pp. 262-268, 2013.

[14] P.V. Parimi, W.T. Lu, P. Vodo, and S. Sridhar, "Photonic crystals: imaging by flat lens using negative refraction," Nature, Vol. 426, pp. 404-410, 2003.

[15] O. Hess, C. Hermann, and A. Klaedtke, "Finite difference time domain simulations of photonic crystal defect structures," Phys. Stat. Sol., Vol. 197, pp. 605-619, 2003.

[16] W. Kuang, W.J. Kim, and J.O'Brien, "Finite difference time domain method for non-orthogonal unit cell two dimensional photonic crystals," J. lightwave Technol. Vol. 25, pp. 2612-2617, 2007.

[17] C. Luo, S.G. Johnson, J.D. Joannopoulos, and J.B. Pendry, "Subwavelength imaging in photonic crystals," Phys. Rev. B, Vol. 68, pp. 045115 (1-15), 2003.

[18] X. Wang, Z.F. Ren, and K. Kempa, "Unrestricted superlensing in a triangular two dimensional photonic crystal," Opt. Express, Vol. 12, pp. 2919-2924, 2004.

[19] F. Xia, M. Yun, M. Liu, J. liang, W. Kong, H. Tan, and W. Lv, "Negative refraction subwavelength imaging in a hexagonal two-dimensional annular photonic crystal," J. Appl. Phys. Vol. 113, pp. 013109 (1-4), 2013.

[20] S.R. Dastjerdi, M. Ghanaatshoar, and T. Hattori, "Design and analysis of superlens based on complex two-dimensional square lattice photonic crystal," Chinese Opt. Lett. Vol. 10, pp. 102303 (1-4), 2013.

Somayeh Rafiee Dastjerdi received her B.S. degree in applied physics from Tarbiat Moallem (Kharazmi) University, Tehran, in 2003 and the M.S. and Ph.D. degrees in

photonics from Shahid Beheshti University, Tehran, in 2006 and 2013, respectively. She is currently collaborating with Laser and Plasma Research Institute, Shahid Beheshti University, Tehran and Optoelectronic Research Centre, University of Southampton, Southampton, UK. Her research interests include photonic bandgap materials, plasmonic devices, silicon photonics and metamaterials.

Majid Ghanaatshoar received his B.S. degree in physics from Isfahan University of Technology in 1992, the M.S. degree from Tehran University in 1995 and his Ph.D. degree in condensed matter physics from Shahid Beheshti University, Tehran, in 2002. He is currently engaged as an associate professor of Physics in Laser and Plasma Research Institute, Shahid Beheshti University, Tehran, I.R. Iran. His research interests span solar cells, nanomagnetism, magnetic semiconducrors, photonic bandgap materials, nanophotonics and plasmonics.

Kaveh Delfanazari awarded his Ph.D degree in Engineering from the University of Tsukuba, Japan, where he investigated superconducting terahertz (THz) oscillating devices during his Ph.D work. He is currently a Research Fellow- Project Leader at EPSRC Centre for Photonic Metamaterials, Optoelectronics Research Centre, University of Southampton, UK. His research interests lie in the areas of nanophotonics, Plasmonics, Josephson junctions based superconducting THz oscillating devices, Superconducting Metamaterials including quantum interface devices (SQUID), Millimeter-wave, Microwave and sub-THz.

THIS PAGE IS INTENTIONALLY LEFT BLANK.